Spatiotemporal Chaos in a Simulated Ring of Cardiac Cells

Zhilin Qu, James N. Weiss, and Alan Garfinkel
Department of Medicine (Division of Cardiology), University of California, Los Angeles, California 90095
(Received 11 September 1996)

We recently presented evidence that cardiac fibrillation is a form of spatiotemporal chaos arising via a quasiperiodic transition. To investigate the origin of this quasiperiodicity, we studied reentrant excitation in a ring of cardiac cells. We modified the Beeler-Reuter model, changing the action potential duration (APD) restitution so that it agreed qualitatively with experimental studies. We found that chaos could occur by reentrant excitation, in a transition from quasiperiodicity to spatiotemporal chaos. This occurred only when the APD restitution curve was nonmonotonic. [S0031-9007(97)02407-1]

PACS numbers: 87.22.As, 05.45.+b, 87.10.+e

Reentrant cardiac arrhythmias are disorders of electrical conduction in which waves of excitation repeatedly "reenter" the same or each other's region of tissue [1]. They include the most malignant arrhythmias, especially ventricular tachycardia and ventricular fibrillation, the latter being the leading single cause of death in industrialized countries. In reentrant tachycardias, a single wave of excitation recirculates through the tissue substrate in a periodic manner, whereas in ventricular fibrillation, wave propagation becomes "frenzied and irregular," coherent cardiac conduction and contraction are lost, and death ensues within minutes.

Recent studies have shown that at least some cardiac arrhythmias may be instances of deterministic chaos, describable by low-dimensional maps [2–5]. However, fibrillation has defied low-dimensional description [6], and requires instead a spatiotemporal approach. The subject of spatiotemporal pattern formation in excitable media is now being studied intensely, including reaction-diffusion systems [7], cardiac spatial propagation [8], and other systems. In these systems, phenomena such as spiral waves, spiral meandering, spiral breakup, and "turbulence" have been observed [7]. But, to our knowledge, there has been little attention given to describing how spatiotemporal chaos can occur during reentrant activity in these extended systems. Recent theoretical modeling by partial differential equations [9,10] and coupled map lattices [11] and experimental studies in rings of cardiac tissue [12] give some crucial insights into the instability caused by reentrant excitation. In this Letter, we extend these investigations to study how these instabilities lead to spatiotemporal chaos in a ring of cardiac tissue.

Cardiac dynamics are determined in part by the properties called "restitution," in which the values of key cardiac variables in a given beat depend on variables from the previous beat. The three most important descriptors of the cardiac cycle are (1) action potential duration (APD), the interval from the beginning of the cardiac upstroke to repolarization, (2) diastolic interval (DI), the time from the end of the action potential to the next upstroke, and (3) conduction velocity (CV). These descriptors are related by the two restitution curves: APD restitution (APD versus preceding DI) and local CV restitution (CV versus preceding DI). Most often, APD restitution curves are described as monotonic functions of DI [10,13]; however, several studies [3,4,13] have reported that APD restitution can be nonmonotonic, first increasing to a local maximum, then decreasing to a local minimum, and then increasing gradually to a steady state maximum. This nonmonotonic effect is prominent in human myocardium, where the difference in APD between the local maximum and minimum can be as large as 20–30 ms [13]. Previous studies have shown that with nonmonotonic APD restitution, bifurcations to chaos have been observed in two periodically driven preparations: Purkinje fiber/papillary muscle [3] and small pieces of cardiac tissue [4]. We now study the consequences of such nonmonotonic restitution curves in an autonomous (i.e., not externally forced) situation: reentry in a ring of cardiac tissue, using the Beeler-Reuter (BR) equations [14] as our cardiac cell model. We modified the BR equations to allow a parametric change in APD restitution from monotonic to nonmonotonic.

We assume that the electrical pulse propagates in a continuous one-dimensional ring of tissue (ignoring the microscopic cell structure) with ring length L, which is described by the following partial differential equation [9,10]:

$$C_m \frac{\partial V}{\partial t} = -I_{\mathrm{BR}} + \frac{1}{S_\nu \rho} \frac{\partial^2 V}{\partial x^2}, \qquad (1)$$

where V(mV) is the membrane voltage, $C_m = 1\ \mu\mathrm{F\,cm^{-2}}$ is the membrane capacitance, $S_\nu = 5000\ \mathrm{cm^{-1}}$ is the surface-to-volume ratio, and $\rho = 0.2\ \mathrm{k\Omega\,cm}$ is the tissue resistivity. The units of time and space in Eq. (1) are ms and cm, respectively. $I_{\mathrm{BR}}(\mu\mathrm{A\,cm^{-2}})$ is the total ionic current from the BR model [14]: $I_{\mathrm{BR}} = I_{\mathrm{Na}} + I_{\mathrm{Ca}} + I_{x_1} + I_{K_1}$. $I_{\mathrm{Na}} = (4m^3hj + 0.003)(V - 50)$ is the fast inward sodium current; $I_{\mathrm{Ca}} = 0.09df(V - E_s)$ is the slow inward calcium current, while $E_s = -82.3 - 13.0287 \ln[\mathrm{Ca}]_i$ and the intracellular calcium concentration $[\mathrm{Ca}]_i$(mol/l) satisfies $d[\mathrm{Ca}]_i/dt = -10^{-7} I_{\mathrm{Ca}} + 0.07(10^{-7} - [\mathrm{Ca}]_i)$; $I_{x_1} = \bar{i}_{x_1} x_1$ is the

time-dependent outward potassium current, which is a voltage-dependent function only. m, h, j, d, f, and x_1 are the corresponding gating variables satisfying differential equations of the type: $dy/dt = (y_\infty - y)/\tau_y$, $y_\infty = \alpha_y/(\alpha_y + \beta_y)$, and $\tau_y = 1/(\alpha_y + \beta_y)$. $\alpha_y(\mathrm{ms}^{-1})$ and $\beta_y(\mathrm{ms}^{-1})$ are the corresponding rate constant, which are also functions solely of voltage. Detailed forms of I_{K_1}, $\bar{i}_{x_1}$, α_y, and β_y can be found in Ref. [14]. To simulate the APD restitution properties of real cardiac tissue, we modified the BR model by blocking the time-dependent outward potassium current I_{x_1} in the following way: $I_{x_1} = g_{x_1}(t')\bar{i}_{x_1}x_1$, and

$$g_{x_1}(t') = \begin{cases} 1 - aF(t'), \\ \quad t' \in [0, \mathrm{APD}], & \text{during action potential}, \\ 1 - aG(t'), \\ \quad t' \in [0, \mathrm{DI}], & \text{during diastolic interval}, \end{cases} \tag{2}$$

where $F(t') = G(\mathrm{DI}) + \int_0^{t'} m^3hj\theta(x_1)\,dt'$ and $G(t') = F(\mathrm{APD})\exp(-t'/T)$, and t' is the local time variable. We set $T = 0.1$ ms and $\theta(x) = e^{-800(x-0.28)^2}$. By changing a in Eqs. (2) we can obtain different shapes of APD restitution curves, which is similar to the manner in which restitution properties are changed in Ref. [15]. We use -60 mV as our threshold between action potential ($V > -60$ mV) and diastolic state ($V < -60$ mV). In Fig. 1 we show the APD restitution curves of the modified BR model for different values of a. For small a the APD restitution is a monotonic function, but for a greater than a critical value ($\approx$0.4) it becomes nonmonotonic. The nonmonotonic APD restitution qualitatively resembles experimental data (Fig. 1, inset). We emphasize that we replicated the experimental APD restitution curve phenomenologically since its ionic mechanism [16] is too complex to incorporate into the BR model.

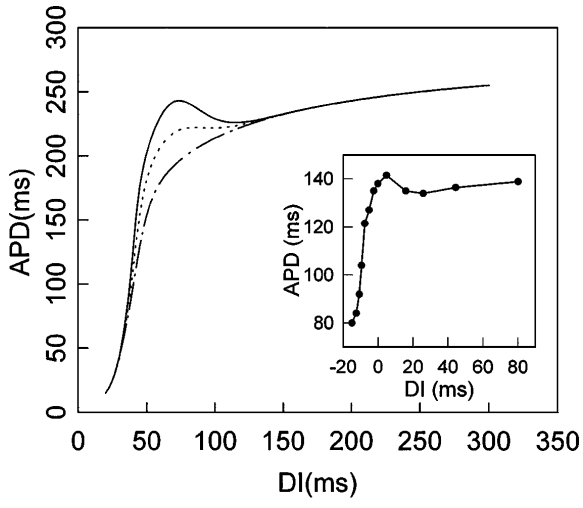

FIG. 1. APD restitution curves of the modified BR model with different values of a: dotted-dashed ($a = 0$, original BR model); dotted ($a = 0.4$); solid ($a = 0.75$). Inset shows an experimental APD restitution curve (data taken from Ref. [4]).

As shown by previous studies [9–11], a circulating wave in a ring of cardiac tissue is periodic when the ring circumference is sufficiently long. When the ring length L is shortened to a critical value, the periodic circulating wave loses its stability via a Hopf bifurcation, and the system will go into a quasiperiodic regime. If L is shortened further to another critical value, conduction failure occurs. In our study, we found that, if the restitution curve of the cell was monotonic, the behavior of the system was identical to that reported by others [9–11]: from periodic circulation to a quasiperiodic regime and then to circulation failure as the ring length was shortened. However, if the restitution curve is nonmonotonic, spatiotemporal chaos occurs after the quasiperiodic regime, and before the circulation failure. Figure 2 shows the phase diagram of the system in a-L parameter plane, obtained by repeated integrating Eq. (1). The phase diagram consists of five regions: stable period 1 circulation (P1); quasiperiodic motion when APD restitution is monotonic (QP1); quasiperiodic motion when APD restitution is nonmonotonic (QP2); spatiotemporal chaos (STC); and circulation failure (F). The transition to chaos always occurs via the QP2 motion when $a > 0.4$. From Figs. 1 and 2 we conclude that *chaos is observed in a ring of cardiac tissue only when the restitution curve is nonmonotonic.*

The quasiperiodic dynamics of this system can be readily seen in first-return maps of the APD. Figure 3(a) shows a quasiperiodic attractor in QP1, and Fig. 3(b) shows a quasiperiodic attractor in QP2. The main difference between QP1 and QP2 is the amplitude of oscillation. QP1 behavior is produced by a monotonic restitution curve (thus, this behavior is the analog of the quasiperiodicity seen in Refs. [9–11]). QP2 behavior, on the other hand, is produced by nonmonotonic restitution. In the curves in Fig. 1, it is the *valley* in the restitution curve, constraining the system, which results in QP2 motion. As

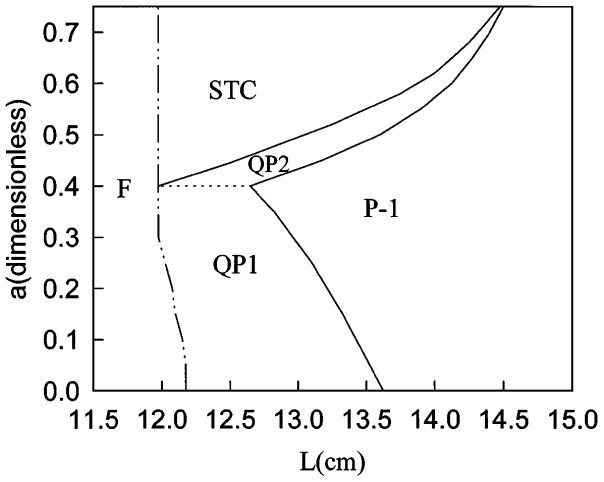

FIG. 2. Phase diagram in a-L plane. P1: period one; QP1: quasiperiodicity, type 1; QP2: quasiperiodicity, type 2; STC: spatiotemporal chaos; F: circulation failure.

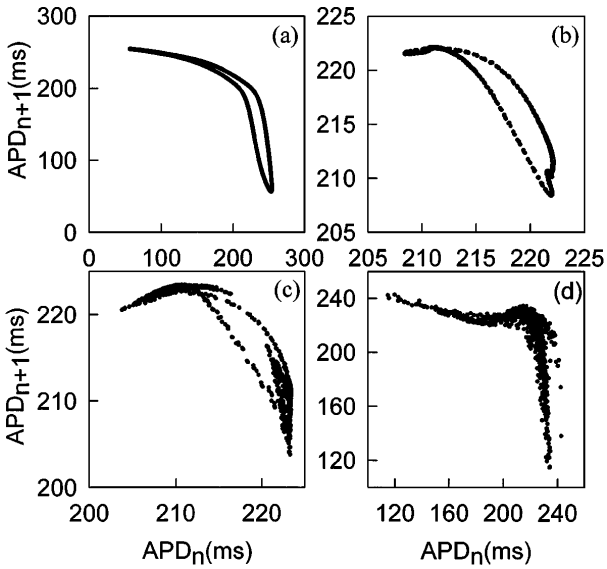

FIG. 3. First-return maps of APD for $L = 12.75$ cm and (a) $a = 0.2$, (b) $a = 0.45$, (c) $a = 0.465$, (d) $a = 0.6$.

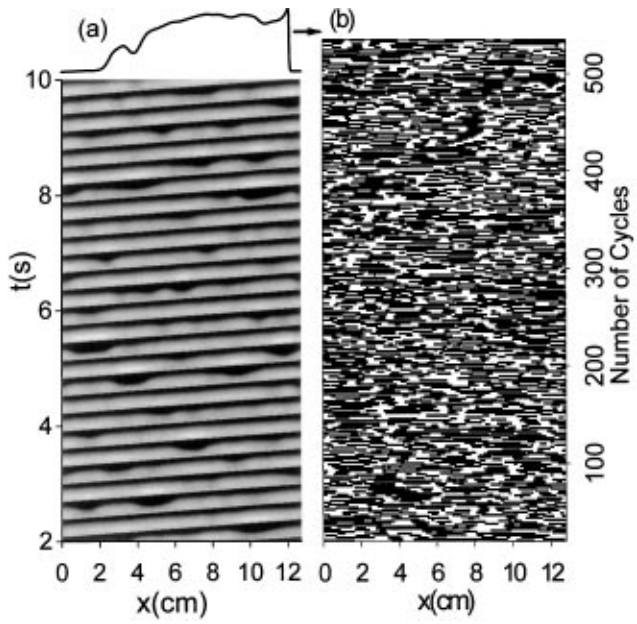

FIG. 4. (a) Gray-scale plot of spatiotemporal evolution of voltage V for $a = 0.6$ and $L = 12.75$ cm. The top is the plot of voltage as a function of space at time $t = 10$ s. The arrow indicates the direction of propagation of the electrical wave along the ring. (We cannot see the wave front variation in this gray-scale plot because it is too small to show up in such a plot; however, the variation of wave front is demonstrated in Fig. 5 by CV variation). (b) Spatiotemporal distribution of the APD versus cycle number for the same parameters as in (a). Pixels are black for APD $>$ 227 ms and white for APD $<$ 227 ms. The abscissa is the spatial distance along the ring, and the ordinate is the number of cycles during reentry.

a becomes larger, however, the motion of the system becomes progressively more violent, and the oscillation can no longer be constrained to the valley region [Figs. 3(c) and 3(d)].

So far, we have discussed only the temporal properties of the system. What is its spatial behavior? Figure 4(a) is a gray-scale plot of spatiotemporal evolution of the voltage between 2 s and 10 s, which shows irregularities in both wavelength and wave form in the STC regime ($a = 0.6, L = 12.75$ cm). To emphasize the spatiotemporal irregularity we plot the spatiotemporal distribution of the APD for a much longer period (over 500 cycles) in Fig. 4(b) for the same parameters as in Fig. 4(a). The violent spatiotemporal irregularity is illustrated much more prominently than in Fig. 4(a). Figure 5 shows a space plot of CV and APD for several cycles. Figures 5(a) and 5(b), for the STC regime ($a = 0.6$), show that CV and APD (indicated by solid lines) along the ring are totally irregular in space and time. To examine the sensitivity of the system to perturbations (a hallmark of chaos), we gave a short perturbation [the dotted sharp peak (indicated by an arrow) in Fig. 5(a)] during steady state conduction, transiently increasing conduction velocity (by increasing I_{Na}), in a very narrow space interval [10 cm, 10.25 cm]. The dotted lines show that after the perturbation, CV and APD values diverged from their original values, first in a local area, and then throughout the whole space, after no more than 10 cycles. Thus the perturbations were amplified both in space and time, indicating that the dynamics of the system is spatiotemporal rather than temporal. For comparison, we performed the same perturbation, with the parameters in the QP1 regime ($a = 0.2, L = 12.75$ cm). With the identical perturbations, the effect on the evolution of APD and CV [Figs. 5(c) and 5(d)] was barely observable.

After determining that our data sets were sufficiently low dimensional by the false nearest neighbors method [17], we calculated Lyapunov exponents by the method of Ref. [18], for the four data sets shown in Fig. 3. In the quasiperiodic regime [Fig. 3(a)] the largest exponent was 0.005 ms^{-1}, not significantly different from zero, whereas in chaotic regime, the largest exponents varied between 0.1 and 0.12 ms^{-1}.

We have demonstrated that the spatiotemporal chaos can arise in an excitable medium in a one-dimensional ring. A novel aspect of this finding is that the chaos arises from a single wave that continually reenters the same regions [see Fig. 4(a)]. This type of chaos is therefore more relevant to reentrant cardiac arrhythmias than chaos arising from periodic external forcing. The presence of chaos, and the particular form that it takes, depends upon the restitution curves for APD and CV. If CV were constant, the time to the next excitation of a given cell would be constant. In this case, the routes to chaos that occur are those that are observed for a single cell with periodic forcing [3,4]. However, in a spatiotemporal system there is always some variability of CV, which will induce spatial complexity by accelerating or retarding the impulse arrival time. These oscillations in CV, coupled to the oscillations in APD produced by restitution

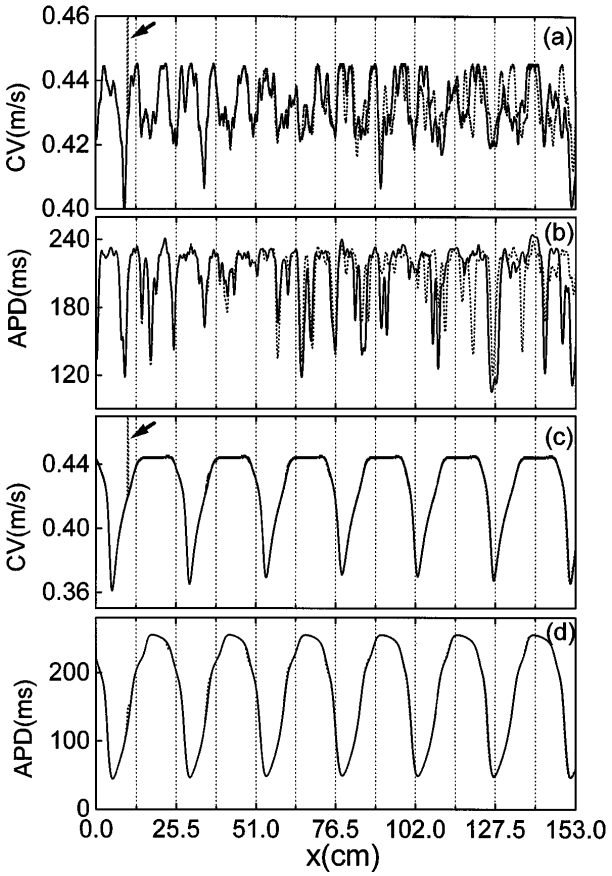

FIG. 5. Spatial distribution and sensitivity to perturbations of CV and APD during reentry for $L = 12.75$ cm. Solid and dotted lines show their evolution during reentry without and with the perturbation, respectively. The perturbation are indicated by the arrows. The vertical dotted grid lines mark the ring circumference. (a) and (b) $a = 0.6$; (c) and (d) $a = 0.2$. Note that the solid and dotted lines diverge after the perturbation in (a) and (b) but remain superimposed in (c) and (d).

characteristics, result in spatiotemporal quasiperiodicity. The shape of the APD restitution curve is critical: if the slope is everywhere less than 1, the quasiperiodicity is transient, and reentry either stabilizes or terminates, depending on the ring length. If the slope is greater than 1, quasiperiodicity becomes sustained at some ring lengths [10] and if, in addition, the APD restitution curve is nonmonotonic, a quasiperiodic transition to chaos is generated.

The most important cardiac arrhythmias, from the clinical point of view, are reentrant waves that take place in two- or three-dimensional tissue, as opposed to the one-dimensional ring studied here. However, we have recently found evidence that fibrillation is a form of spatiotemporal chaos that arises from a quasiperiodic transition [19]. These one-dimensional simulations provide insight into the origins of quasiperiodicity which may be relevant to higher dimensional settings. In atrial and ventricular fibrillation, multiple reentrant spiral waves meander and break up in two- and three-dimensional segments of cardiac tissue [8]. In simulations, the transition from stable spiral wave propagation to spiral meander has been shown to be a Hopf bifurcation to quasiperiodicity. The importance of the specific characteristics of APD and CV restitution curves suggests that they may be useful therapeutic targets for prevention of unstable forms of reentry that underlie cardiac fibrillation.

This research was supported in part by Grant No. P50-HL52319 from the National Institutes of Health.

[1] D. P. Zipes and J. Jalife, *Cardiac Electrophysiology: from Cell to Bedside* (W. B. Saunders, Philadelphia, 1995), 2nd ed.
[2] A. Garfinkel *et al.,* Science **257**, 1230 (1992); F. X. Witkowski *et al.,* Phys. Rev. Lett. **75**, 1230 (1995).
[3] D. R. Chialvo *et al.,* Nature (London) **343**, 653 (1990).
[4] M. Watanabe *et al.,* Circ. Res. **76**, 915 (1995).
[5] D. R. Chialvo and J. Jalife, Nature (London) **330**, 749 (1987); M. R. Guevara *et al.,* Science **214**, 1350 (1981).
[6] A. T. Winfree, *When Time Breaks Down* (Princeton University Press, Princeton, 1987); D. T. Kaplan and R. J. Cohen, Circ. Res. **67**, 886 (1990).
[7] H. L. Swinney and V. I. Krinsky, *Waves and Patterns in Chemical and Biological Media* (MIT/North-Holland, Cambridge/Amsterdam, 1992); Q. Ouyang and J. M. Flesselles, Nature (London) **379**, 143 (1996); K. I. Agladze *et al.,* Nature (London) **308**, 834 (1984); M. Markus *et al.,* Nature (London) **371**, 402 (1994).
[8] J. M. Davidenko *et al.,* Nature (London) **355**, 349 (1992); A. Karma, Phys. Rev. Lett. **71**, 1103 (1993); A. T. Winfree, Science **266**, 1003 (1994); R. A. Gray *et al.,* Science **270**, 1223 (1995).
[9] W. Quan and Y. Rudy, Circ. Res. **66**, 367 (1990); A. Karma *et al.,* Physica (Amsterdam) **73D**, 113 (1994).
[10] M. Courtemanche *et al.,* Phys. Rev. Lett. **70**, 2182 (1993).
[11] H. Ito and L. Glass, Physica (Amsterdam) **56D**, 84 (1992).
[12] L. H. Frame and M. B. Simson, Circulation **78**, 1277 (1988).
[13] M. R. Franz *et al.,* Circ. Res. **53**, 815 (1983); J. M. Morgan *et al.,* J. Am. Coll. Cardiol. **19**, 1244 (1992).
[14] G. W. Beeler and H. Reuter, J. Physiol. **268**, 177 (1977).
[15] A. Karma, Chaos **4**, 461 (1994); B. Y. Kogan *et al.,* Physica (Amsterdam) **50D**, 327 (1991).
[16] J. Zeng *et al.,* Circ. Res. **77**, 140 (1995).
[17] M. B. Kennel *et al.,* Phys. Rev. A **45**, 3403 (1992).
[18] M. Rosenstein *et al.,* Physica (Amsterdam) **65D**, 117 (1993).
[19] A. Garfinkel *et al.,* Circulation (Suppl. I) **90**, I-541 (1994); J. Clin. Invest. **99**, 305 (1997).